Quaternary International 493 (2018) 252–257

Contents lists available at ScienceDirect

Quaternary International

journal homepage: www.elsevier.com/locate/quaint

The cause of extremely high magnetic susceptibility of the S5S1 paleosol in the central Chinese Loess Plateau

Hao Lu[a,b], Jia Jia[a,*], Youjun Wang[a], Qiuzhen Yin[b], Dunsheng Xia[a]

[a] Key Laboratory of West China's Environmental System (Ministry of Education), College of Earth and Environmental Sciences, Lanzhou University, Lanzhou, 730000, China

[b] Georges Lemaître Centre for Earth and Climate Research, Earth and Life Institute, Université Catholique de Louvain, Louvain-La-Neuve, 1348, Belgium

A R T I C L E I N F O

Keywords:
S5S1 paleosol
MIS-13 interglacial
Iron mineralogical proxies
Paleoclimate
Pedogenesis
Chinese Loess Plateau

A B S T R A C T

The paleosol unit S5S1, which corresponds to Marine Isotope Stage (MIS) 13, is the most prominent paleosol layer in the central Chinese Loess Plateau (CLP). S5S1 has extremely high magnetic susceptibility, but it remains uncertain whether this is related to climate or to time (the duration of pedogenesis) due to the anomalously low loess deposition rate. To address this question, we investigate the iron mineralogical properties of the S5S1 paleosol at the Xifeng loess section located in the central CLP. We compare the results of S5S1 with other paleosol units, yielding additional insights into the CLP climatic changes during MIS-13. The results show that magnetic enhancement of S5S1 paleosol is stronger than that of the other paleosol units, which is mainly governed by pedogenic produce fine-grained ferrimagnetic minerals; the maximum value of the goethite concentration compared with hematite in the S5S1 paleosol unit is markedly higher than those in the other paleosol units. The prolonged period of pedogenesis is not main controlling factor that leads to the magnetic enhancement of S5S1 because the concentration of SD/SP has hardly changed compared with other paleosols as with the increasing of magnetic susceptibility. Changes in the ratio of pedogenic hematite to goethite, as well as in magnetic enhancement, indicate that the S5S1 paleosol developed under extremely humid conditions. This extremely humid climate is a main cause that leads to the extremely high magnetic susceptibility.

1. Introduction

The marine isotope stage (MIS) 13 interglacial occurred about 500,000 years ago. It is characterized by cooler Antarctic temperature (Jouzel et al., 2007) (Fig. 1a), a relatively lower CO_2 and CH_4 concentrations (Lüthi et al., 2008; Loulergue et al., 2008) (Fig. 1b), and likely larger global ice volume (e.g., Lisecki and Raymo, 2005) (Fig. 1d), in comparison with other interglacials of the last million years. However, geological records from the central Chinese Loess Plateau (CLP) appear to illustrate a complex pattern, including an extremely strong summer monsoon during MIS-13 (e.g. An et al., 1987; Kukla et al., 1990; Guo et al., 2009), inferred from the occurrence of anomalously high magnetic susceptibility of S5S1 paleosol (Fig. 1c). This appears not as an isolated climatic event as corresponding evidence has been observed in the Indian and African Monsoon Regions. For example, the occurrence of a peak in the planktic oxygen isotope records from the equatorial Indian Ocean (Bassinot et al., 1994) indicates strong Indian Monsoon circulation, and anomalous sapropel (Sa) in the Mediterranean following high floods of Nile river indicates unusually heavy monsoon rainfall over Africa (Rossignol-Strick et al., 1998). The corresponding paleosol of the Serbian loess in the Southeastern European is also the most developed (Bronger, 2003; Buggle et al., 2009; Marković et al., 2009, 2012, 2015). Different proposals have been made to explain the strong summer monsoon during MIS-13, for example, the tectonic uplift of the Tibetan Plateau (An et al., 1990; Xiao and An, 1999) and hemisphere asymmetry in ice volume development (Guo et al., 2009). Climate models of different complexities have also been used to investigate the response of the East Asian Summer Monsoon to insolation, greenhouse gases concentration, ice sheets and the size of Tibetan Plateau during MIS-13 (Yin et al., 2008, 2009; Muri et al., 2012). Recently, a climate-soil combined model was used to simulate the soil formation of this interglacial on the CLP (Finke et al., 2017). In the meantime, regional diversity exists in the relative intensity of the S5S1 soil formation. Specifically, different from the central and eastern CLP, the S5S1 paleosol is weakly developed in the western CLP while the S4 paleosol (developed during MIS-11) is the most developed in the Quaternary loess-paleosol sequences (Chen and Zhang, 1993; Sun et al., 2006a; Shi et al., 2013) (Fig. 1c). This

* Corresponding author. Key Laboratory of West China's Environmental System (Ministry of Education), College of Earth and Environmental Sciences, Lanzhou University, Lanzhou, 730000, China.

E-mail address: jiaj@lzu.edu.cn (J. Jia).

https://doi.org/10.1016/j.quaint.2018.05.046
Received 14 February 2018; Received in revised form 23 May 2018; Accepted 31 May 2018
Available online 31 May 2018
1040-6182/

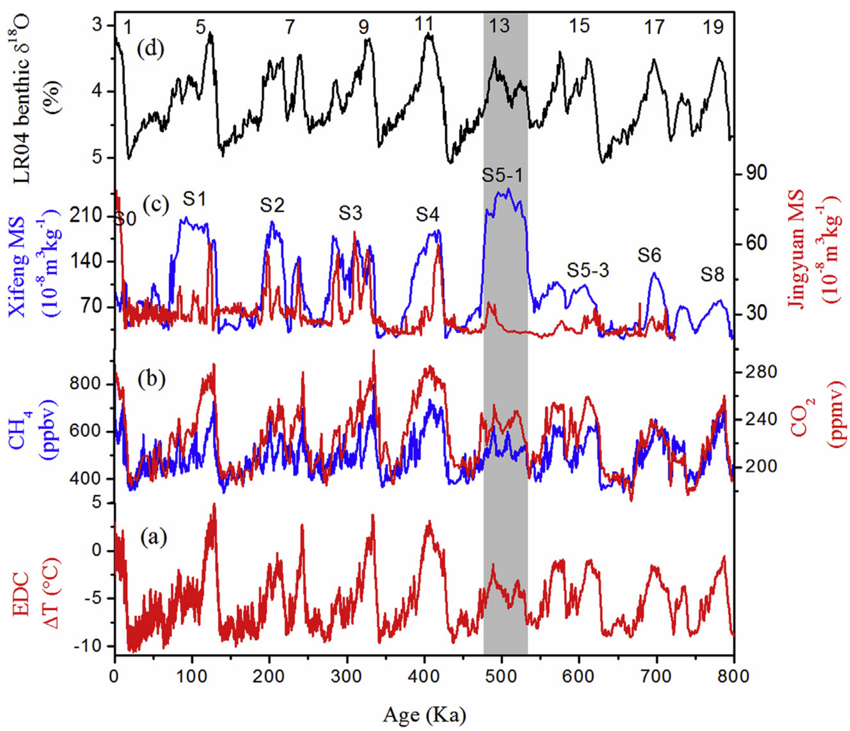

Fig. 1. Comparison of the China loess proxies of East Asian summer monsoon with relevant ice and marine records. (a) Antarctic temperature (EDC) record (red) (Jouzel et al., 2007); (b) Antarctic CH_4 (blue) (Loulergue et al., 2008) and CO_2 records (red) (Lüthi et al., 2008); (c) loess magnetic susceptibility at Xifeng (blue) (Guo et al., 2009) and Jingyuan (red) (Sun et al., 2006a) with the major paleosol units labeled; (d) Marine $\delta^{18}O$ record (black) (Lisiecki and Raymo, 2005) with the interglacial oxygen isotope stages (MIS) labeled at the top part. Grey frame denote the proxies for which MIS-13 can be considered as typical from an amplitude signal point of view. (For interpretation of the references to color in this figure legend, the reader is referred to the Web version of this article.)

discrepancy has been explained by regional inconsistencies in timing of climate shift relative to the mid-Brunhes epoch (Sun et al., 2006a).

The magnetic susceptibility of the loess-paleosol sequences has been widely used to reconstruct paleoclimate variations corresponding to the loess and paleosol alternations, with high magnetic susceptibility in paleosol units contrasting with low values in loess units (Liu, 1985; Kukla and An, 1989; An et al., 1990). The product of newly-generated, fine-grained and strongly-magnetic particles that are related to pedogenic activity have been widely regarded as the major factor enhancing magnetic susceptibility in the soil units (e.g., Zhou et al., 1990; Maher and Thompson, 1991). In addition, specially, material leaching also can lead to magnetic susceptibility enhancement through the enrichment of strongly magnetic particles with time (Singer et al., 1996; Vidic and Verosub, 1999; Vidic et al., 2004). Considering the low loess deposition rate during this interglacial and therefore the prolonged period of pedogenesis, one may assume that the extremely high magnetic susceptibility in the S5S1 paleosol resulting from time effect (Han et al., 1998; Bronger, 2003; Marković et al., 2011). In particular, there is a relatively low magnetic susceptibility in the western CLP loess sequences, where the deposition rate is about twice that in the central CLP, or even more (Sun et al., 2010); in turn, the duration of the soil formation is much shorter. Therefore, it is important to determine in which degree the extremely high magnetic susceptibility of S5S1 represents a climate signal.

It has been widely observed that iron minerals are sensitive to pedogenesis (Schwertmann, 1993; Inda et al., 2013; Hu et al., 2016). In this study, we will investigate the iron mineralogical properties of S5S1 magnetic minerals in the central CLP, and compare them with those of other paleosol units to provide additional insights into the CLP climatic changes during MIS-13.

2. Materials and methods

2.1. The site and sampling

Samples were collected from a profile at Xifeng (XF: Fig. 2) located in the central CLP at 35°46′N, 107°41′E, 1345 m a.s.l. The site is presently characterized by semi-arid climate, with mean annual temperature (MAT) of ~8.3 °C and precipitation (MAP) of ~560 mm. The XF profile is one of the most representative loess stratigraphy sites in the central CLP, with 33 documented loess and paleosol alternations throughout Quaternary (Kukla and An, 1989). The whole profile reaches about 170 m in thickness, of which the upper 62.9 m was selected for the present study. This includes the sequences from S0 (Holocene) to S6 (MIS-17). With a 10-cm sampling interval, 630 samples were collected. Field observations show that S5S1, which is distinguished by its great thickness (2.3 m), dark color, and well-developed clay coatings, is the most developed paleosol unit.

2.2. Magnetic measurement

All samples were air-dried; 5 g of sediment was packed into $2 \times 2 \times 2\ cm^3$ nonmagnetic plastic boxes. Magnetic susceptibility was measured, low frequency (χ_{lf}) with 470 Hz, high frequency (χ_{hf}) with 4700 Hz, by Bartington MS2 meter. The absolute frequency dependent susceptibility (χ_{fd}) was calculated $\chi_{fd} = (\chi_{lf} - \chi_{hf})$. Anhysteretic remanent magnetization (ARM) was measured in the minispin magnetometer after magnetization with a DTECH AF demagnetizer, the peak AF field used was 100 mT and the DC bias was 50 μT. ARM was then normalized by the bias field to obtain ARM susceptibility (χ_{ARM}). Isothermal remanent magnetization (IRM) was acquired with a MMPM10 pulse magnetizer and the induced remanence after 1 T and one reverse 300 mT were measured in a JR-6A spinner magnetometer, respectively. The IRM acquired in the maximum field of 1 T is defined as the saturation isothermal remanent magnetization (SIRM), and the reverse 300 mT is expressed as IRM_{-300mT}. The "hard" isothermal remanent magnetization (HIRM) is defined as HIRM = (SIRM + IRM_{-300mT})/2.

2.3. Diffuse reflectance spectroscopy measurements and calculations

46 samples were selected from the XF profile to quantify the mass concentrations of hematite and goethite. The samples were ground to below 200-mesh with an agate mortar. Ground samples were made into slurry on a glass micro-slide with distilled water, smoothed, and dried slowly at room temperature. The diffuse reflectance spectrum (DRS)

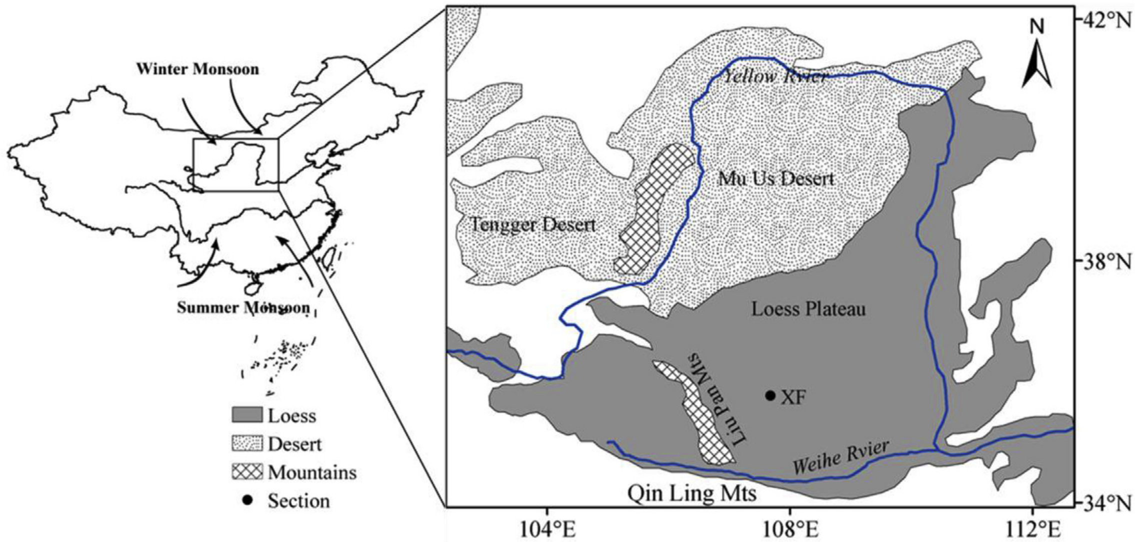

Fig. 2. Location of the CLP in China, directions of monsoon circulation systems (modified from Sun et al., 2010), and location of XF profile.

was obtained over the range from 400 to 700 nm at 1 nm intervals using a Perkin Elmer Lambda 950 spectrophotometer. The color index, redness, was calculated using the standard color band (Judd and Wyszecki, 1975). According to the method of Long et al. (2011), the linear regression model linking the hematite concentration (Hm) and redness is as follows: Hm (%) = 0.05 × redness − 1.15. The concentration of free iron oxides (Fed) was determined using the citrate/bicarbonate/dithionite (CBD) method and finally the formula Gt (%) = 1.59 × (Fed − Hm (%)/1.43) (Torrent et al., 2007) yielded the concentration of goethite (Gt).

3. Results

3.1. Magnetic parameters in the XF profile

The χ_{lf} (Fig. 3a) shows that the higher values correspond to paleosol units and the lower values correspond to loess units, the variation of which is consistent with loess and paleosol alternations. The χ_{lf} value of the S5S1 paleosol reaches $253.90 \times 10^{-8}\,m^3\,kg^{-1}$, and is obviously higher than those of the other paleosol units (Fig. 3a and Table 1). The χ_{fd} indicates the concentration of the superparamagnetic (SP) ferrimagnetic minerals produced during pedogenesis, which can be used to reflect the intensity of pedogenesis (Liu et al., 2007a). The variation of the χ_{fd} is similar to that of the χ_{lf} (Fig. 3b). The peak χ_{fd} value of S5S1 ($33.2 \times 10^{-8}\,m^3\,kg^{-1}$) is the highest and is about double of those of the S6 paleosol (max. $16.10 \times 10^{-8}\,m^3\,kg^{-1}$) (Fig. 3b and Table 1),

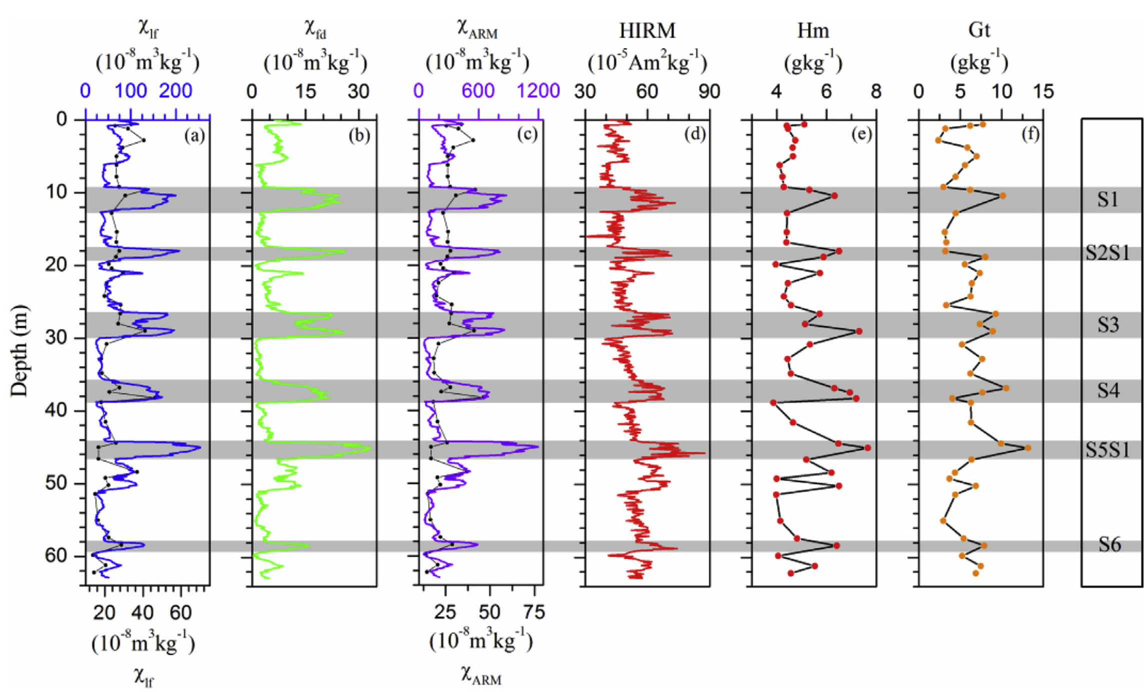

Fig. 3. The variations for magnetic parameters, concentration of hematite and goethite in the XF profile. The black dotted lines are post-CBD χ_{lf} and post-CBD χ_{ARM}, respectively, in Fig. 3a and c. The grey shadows indicate the paleosol units.

Table 1
The comparison of magnetic parameters and hematite/goethite for typical paleosol units in XF profile. The S5S1 paleosol unit is labeled in red.

Paleosol Units	χ_{lf} ($10^{-8}m^3\cdot kg^{-1}$)	χ_{fd} ($10^{-8}m^3\cdot kg^{-1}$)	χ_{ARM} ($10^{-8}m^3\cdot kg^{-1}$)	HIRM ($10^{-5}Am^2kg^{-1}$)	Hm (gkg^{-1})	Gt (gkg^{-1})
S1	199.50	24.90	879.19	73.23	6.32	10.13
S2S1	207.50	26.20	813.60	71.47	6.50	8.01
S3	196.10	25.90	860.70	71.90	7.31	9.27
S4	169.60	21.60	706.28	68.12	7.19	10.53
S5S1	253.90	33.20	1197.83	87.55	7.65	13.17
S6	129.80	16.10	588.61	74.24	6.40	7.88

indicating that the concentration of the SP ferrimagnetic minerals is higher in S5S1 than in other paleosol units. The parameter χ_{ARM} is particularly sensitive to the concentration of single domain (SD) ferrimagnetic grains (Thompson and Oldfield, 1986) and ranges from $45.10 \times 10^{-8}\,m^3\,kg^{-1}$ to $1197.83 \times 10^{-8}\,m^3\,kg^{-1}$, again having a similar variation as the χ_{lf} and χ_{fd} (Fig. 3a and b). The maximum value is $1197.83 \times 10^{-8}\,m^3\,kg^{-1}$ in S5S1, much higher than in S2S1 (max. $813.60 \times 10^{-8}\,m^3\,kg^{-1}$), S3 (max. $860.70 \times 10^{-8}\,m^3\,kg^{-1}$) and S4 (max. $706.28 \times 10^{-8}\,m^3\,kg^{-1}$) (Fig. 3c and Table 1). This indicates that the concentration of the SD ferrimagnetic grains is the highest in S5S1. As shown by the black dotted lines of Fig. 3a and c, after the CBD extraction the samples exhibit a narrow range of χ_{lf} ($13.87 \times 10^{-8}\,m^3\,kg^{-1}$ to $41.62 \times 10^{-8}\,m^3\,kg^{-1}$) and of χ_{ARM}, which is very close to the lithologic susceptibility. Comparison of the pre-CBD and post-CBD χ_{lf} values provides further evidence that the pedogenic signal is removed by CBD treatment and that the χ_{ARM} of post-CBD samples reflects the eolian magnetic mineralogy.

HIRM is generally used as a proxy for the concentrations of hematite and goethite, but it is more sensitive to hematite, with low sensitivity to goethite, mainly because goethite does not reach saturation under 7 T magnetic fields (King and Channell, 1991; Maher et al., 2004; Liu et al., 2007b; Nie et al., 2010). Compared with other proxies, HIRM has higher-frequency variability, and a decreasing trend from bottom to top (Fig. 3d). The fluctuation frequency of HIRM values was greater than other magnetic parameters (from $30.20 \times 10^{-5}Am^2kg^{-1}$ to $87.55 \times 10^{-5}Am^2kg^{-1}$), with the maximum value occurring in S5S1 (Fig. 3d and Table 1), indicating that the concentration of hematite is higher in S5S1 than in other paleosol units.

3.2. Hematite and goethite

Hematite and goethite are common minerals in soil, and are products of silicate mineral weathering. Their distribution and concentration in soil are closely related to the climate and environment (Schwertmann, 1971). The variations of hematite and goethite concentrations are consistent with the χ_{lf} and χ_{fd} values (Fig. 3a and b), showing high values in the paleosol and low values in the loess (Fig. 3e and f). In the S5S1 unit, the maximum goethite concentration is about 13.17 gkg^{-1} (Fig. 3f and Table 1), which is obviously higher than that of other paleosol units, while the maximum hematite concentration is 7.65 gkg^{-1} and similar to 7.19 gkg^{-1} for S4 and 7.31 gkg^{-1} for S3 (Fig. 3e and Table 1).

4. Discussion

Magnetic parameters (χ_{lf}, χ_{fd}, χ_{ARM}) indicate a large number of fine-grained ferrimagnetic minerals lead to S5S1 paleosol magnetic enhancement, which is stronger than that of the other paleosols (Fig. 3a–c). While this magnetic enhancement may be as result of prolonged period of pedogenesis because the average loess sedimentation rate of S5S1 was significantly lower than that of other paleosol units at XF (Guo et al., 2009), similarly to Luochuan, Lingtai (Sun et al., 2006b) and other profiles, a similar viewpoint has also been put forward for the strongly developed paleosol V-S5 of Serbian loess (Bronger, 2003; Marković et al., 2011), and the climate is in a relatively cold interglacial which seems unlikely to produce a large number of summer rainfall in theory (Yin et al., 2008). Meanwhile, the investigation of the S1 paleosol development has shown that deposition rate of the soil in the central CLP is significantly lower than the soil pedogenic rate (Feng and Wang, 2006). The loess can therefore develop into mature soils in equilibrium with the local climate. While it can be inferred that the S5S1 paleosol, the deposition rate of the soil is lower than that of S1 paleosol, has developed into a soil that is in equilibrium with the local climate, it is possible that the magnetic mineral composition, concentration and magnetic grain size of soil could change if prolonged period of pedogenesis occurs after this equilibrium (Tramp et al., 2004), which may lead to soil magnetic enhancement. Therefore, we need to discuss the iron mineralogical properties of S5S1, which will help us to understand the influence factors of magnetic enhancement.

As far as the grain size of magnetic minerals, the magnetic enhancement of paleosols was attributed to pedogenic produce the fine-grained (SP + SD) maghemite (e.g., Zhou et al., 1990; Deng et al., 2004; Liu et al., 2004). To infer the extent that the prolonged period of S5S1 paleosol impacts the pedogenic produce grain size of magnetic minerals, we use the $\Delta\chi_{ARM}/\chi_{fd}$ ratio to reflect the variation in the relative content of SD/SP grain sizes, where $\Delta\chi_{ARM}$ is calculated as Pre-CBD χ_{ARM} − Post-CBD χ_{ARM}, which is as excluding the original eolian magnetic mineralogy. However, compared with the increasing values of χ_{lf}, the values of $\Delta\chi_{ARM}/\chi_{fd}$ change very little (Fig. 4a). The $\Delta\chi_{ARM}/\chi_{fd}$ values for the S5S1 paleosol unit are very similar to those of other paleosol units, indicating that the relative concentration of SD/SP hardly any change with the increasing of magnetic susceptibility. This signifies that the prolonged period of pedogenesis is not mainly factor that impact the magnetic enhancement on S5S1 paleosol because previous researchers found that the grain size of maghemite increased with time of duration in the laboratory from the initial values in the SP region to others in the SD region (Liu et al., 2008; Torrent et al., 2010), which could lead to the variation in the relative content of SD/SP with the increasing of the duration of pedogenesis, especially, for the prolonged period of pedogenesis.

The hematite is favored by high temperatures and a short period of limited rainfall with the raid release of iron under neutral to slightly acidic conditions, and it is sensitive to temperature (Schwertmann, 1971, 1983; Gao et al., 2018). As shown in Fig. 4b, there is a linear positive correlation between the concentration of hematite and pedogenic magnetite, indicating that pedogenic magnetite and hematite were formed simultaneously, while the S5S1 hematite concentration reached a maximum value only slightly higher than those of S4 and S3 as shown in Fig. 3e and Table 1. Whereas goethite, which predominates in soils that are cool, moist and rich in organic matter and forms directly from a variety of Fe source via source (Schwertmann, 1971, 1983), does not appear to be temperature sensitive and is favored by

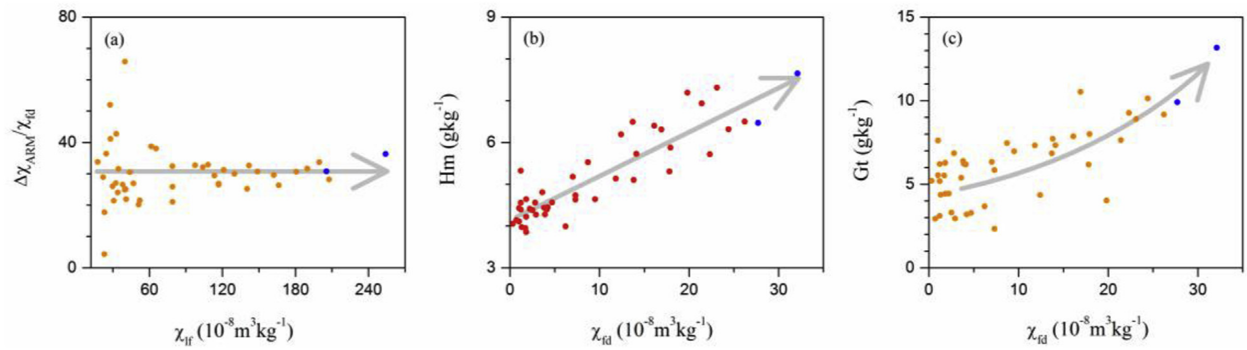

Fig. 4. Relationship between (a) $\Delta\chi_{ARM}/\chi_{fd}$ and χ_{lf}; (b) hematite and χ_{fd}; (c) goethite and χ_{fd}. The blue dots represent S5S1 samples. (For interpretation of the references to color in this figure legend, the reader is referred to the Web version of this article.)

humid conditions. Kämpf and Schwertmann (1983) showed that the proportion of hematite compared to goethite increases with increasing mean annual air temperature, whereas the proportion of goethite increases with increasing excess moisture, i.e., rainfall minus evapotranspiration. There is non-linear correlated with the pedogenic concentration of magnetite, the rate of goethite formation gradually increased with pedogenic intensity; in particular, the pedogenic environment of the S5S1 paleosol was more favorable to goethite formation than to hematite (Fig. 4c), at the same time, the maximum value of the goethite concentration in the S5S1 paleosol unit was markedly higher than those in the other paleosol units (Fig. 3f and Table 1), indicating that the S5S1 paleosol pedogenic environment was extremely humid.

In summary, the magnetic enhancement of S5S1 paleosol in the XF profile is dominated by extremely humid environment rather than the prolonged period of peodegenesis. This is in line with the finding based on climate-soil combined models that the strong developed MIS-13 soil is mainly due to the higher accumulated precipitation surplus during this interglacial (Finke et al., 2017).

5. Conclusions

Magnetic enhancement of the S5S1 paleosol unit can be ascribed to produce a large number of fine-grained ferrimagnetic minerals. The prolonged period of pedogenesis is not mainly factor that impact the magnetic enhancement on S5S1 paleosol. Changes in the ratio of pedogenic hematite to goethite, and in magnetic enhancement, indicate that the S5S1 paleosol unit developed under extremely humid conditions. This extremely humid climate is a main cause that leads to the extremely high magnetic susceptibility.

Acknowledgements

This study was funded by National Natural Science Foundation of China (No. 41401046), the Open Foundation of MOE Key Laboratory of Western China's Environmental System, Lanzhou University and the Fundamental Research Funds for the Central Universities (Grant No. lzujbky-2016-264, lzujbky-2017-it89 and lzujbky-2017-kl01) and China Scholarship Council under the file number 201706180099.

References

An, Z.S., Liu, T.S., Lu, Y.C., Porter, S.C., Kukla, G., Wu, X.H., Hua, Y.M., 1990. The long-term paleomonsoon variation recorded by the loess-paleosol sequence in central China. Quat. Int. 7–8, 91–95.

An, Z.S., Liu, T.S., Zhu, Y.Z., Sun, F., 1987. The paleosol complex S5 in the China Loess Plateau – a record of climatic optimum during the last 1.2 Ma. Geojournal 15, 141–143.

Bassinot, F.C., Labeyrie, L.D., Vincent, E., Quidelleur, X., Shackleton, N.J., Lancelot, Y., 1994. The astronomical theory of climate and the age of the Brunhes-Matuyama magnetic reversal. Earth Planet Sci. Lett. 126, 91–108.

Bronger, A., 2003. Correlation of loess–paleosol sequences in East and Central Asia with SE Central Europe: towards a continental Quaternary pedostratigraphy and paleoclimatic history. Quat. Int. 106–107, 11–31.

Buggle, B., Hambach, U., Glaser, B., Gerasimenko, N., Marković, S., Glaser, I., Zöller, L., 2009. Stratigraphy, and spatial and temporal paleoclimatic trends in Southeastern/Eastern European loess–paleosol sequences. Quat. Int. 196, 86–106.

Chen, F.H., Zhang, W.X., 1993. Loess Stratigraphy and Quaternary Glaciation in Gansu-Qinghai Region. Science Press, pp. 1–155.

Deng, C.L., Zhu, R.X., Verosub, K.L., Singer, M.J., Vidic, N.J., 2004. Mineral magnetic properties of loess/paleosol couplets of the central loess plateau of China over the last 1.2 Myr. J. Geophys. Res. 109 B01103.

Finke, P., Yin, Q.Z., Bernardini, N.J., Yu, Y.Y., 2017. Climate-soil model reveals causes of differences between Marine Isotope Stage 5e and 13 paleosols. Geology 46, 99–102.

Feng, Z.D., Wang, H.B., 2006. Geographic variations in particle size distribution of the last interglacial pedocomplex S1 across the Chinese Loess Plateau: their chronological and pedogenic implications. Catena 65, 315–328.

Guo, Z.T., Berger, A., Yin, Q.Z., Qin, L., 2009. Strong asymmetry of hemispheric climates during MIS-13 inferred from correlating China loess and Antarctica ice records. Climate Past 5, 21–31.

Gao, X.B., Hao, Q.Z., Wang, L., Oldfield, F., Bloemendal, J., Deng, C.L., S, Y., Ge, J.Y., Wu, H.B., Xu, B., Li, F.J., Han, L., Fu, Y., 2018. The different climatic response of pedogenic hematite and ferrimagnetic minerals: evidence from particle-sized modern soils over the Chinese Loess Plateau. Quat. Sci. Rev. 179, 69–86.

Han, J.T., Fyfe, W.S., Longstaffe, F.J., 1998. Climatic implications of the S5 paleosol complex on the southernmost Chinese Loess Plateau. Quat. Res. 50, 21–33.

Hu, P.X., Jiang, Z.X., Liu, Q.S., Heslop, D., Roberts, A.P., Torrent, J., Barrón, V., 2016. Estimating the concentration of aluminum-substituted hematite and goethite using diffuse reflectance spectrometry and rock magnetism: feasibility and limitations. J. Geophys. Res. Solid Earth 121, 4180–4194.

Inda, A.V., Torrent, J., Barrón, V., Bayer, C., Fink, J.R., 2013. Iron oxides dynamics in a subtropical Brazilian Paleudult under long-term no-tillage management. Agric. Sci. 70, 48–54.

Jouzel, J., Masson-Delmotte, V., Cattani, O., Dreyfus, G., Falourd, S., Hoffman, G., Minster, B., Nouet, J., Barnola, J.M., Chappellaz, J., Fischer, H., Gallet, J.C., Johnsen, S., Leuenberger, M., Loulergue, L., Luethi, D., Oerter, H., Parrenin, F., Raisbeck, G., Raynaud, D., Schilt, A., Schwander, J., Selmo, E., Souchez, R., Spahni, R., Stauffer, B., Steffensen, J.P., Stenni, B., Stocker, T.F., Tison, J.L., Werner, M., Wolff, E.W., 2007. Orbital and millennial Antarctic climate variability over the past 800,000 years. Science 317, 793–796.

Judd, D.B., Wyszecki, G., 1975. Color in Business, Science and Industry, third ed. John Wiley and Sons Ltd, New York.

Kämpf, N., Schwertmann, U., 1983. Goethite and hematite in a climo-sequence in southern Brazil and their application in classification of kaolinitic soils. Geoderma 29, 27–39.

Kukla, G., An, Z.S., 1989. Loess stratigraphy in Central China. Palaeogeogr. Palaeoclimatol. Palaeoecol. 72, 203–225.

Kukla, G., An, Z.S., Melice, J.L., Gavin, J., Xiao, J.L., 1990. Magnetic susceptibility record of Chinese loess. Trans. R. Soc. Edinb. Earth Sci. 81, 263–288.

King, J., Channell, J., 1991. Sedimentary magnetism, environmental and magnetostratigraphy. Rev. Geophys. 39, 358–370.

Lisiecki, L.E., Raymo, M.E., 2005. A Pliocene-Pleistocene stack of 57 globally distributed benthic δ^{18}O records. Paleoceanography 20. https://doi.org/10.1029/2004PA001071.

Liu, Q.S., Jackson, M.J., Banerjee, S.K., Maher, B.A., Deng, C.L., Pan, Y.X., Zhu, R.X., 2004. Mechanism of the magnetic susceptibility enhancements of the Chinese loess. J. Geophys. Res. 119 B12107. http://doi.org/10.1029/2004jb003249.

Liu, Q.S., Barron, V., Torrent, J., Eeckhout, S.G., Deng, C.L., 2008. Magnetism of intermediate hydromaghemite in the transformation of 2-line ferrihydrite into hematite and its paleoenvironmental implication. J. Geophys. Res. 113. https://doi.org/10.1029/2007JB225207.

Liu, Q.S., Deng, C.L., Torrent, J., Zhu, R.X., 2007a. Review of recent developments in mineral magnetism of the Chinese loess. Quat. Sci. Rev. 26, 368–385.

Liu, Q.S., Roberts, A.P., Torrent, J., Horng, C.S., Larrasoaña, J.C., 2007b. What do the HIRM and S-ratio really measure in environmental magnetism? Geochem. Geophys. Geosyst 8, Q09011. http://dx.doi.org/10.1029/2007GC001717.

Liu, T.S., 1985. Loess and Environment. Science Press, pp. 303–336.
Long, X.Y., Ji, J.F., Balsam, W., 2011. Rainfall-dependent transformations of iron oxides in a tropical saprolite transect of Hainan Island, South China: spectral and magnetic measurements. J. Geophys. Res. 116. https://doi.org/10.1029/2010JF001712.
Loulergue, L., Schilt, A., Spahni, R., Masson-Delmotte, V., Blunier, T., Lemieux, B., Barnola, J.M., Raynaud, D., Stocker, T.F., Chappellaz, J., 2008. Orbital and millennial-scale features of atmospheric CH_4 over the past 800,000 years. Nature 453, 383–386.
Lüthi, D., Le, F.M., Bereiter, B., Blunier, T., Barnola, J.M., Siegenthaler, U., Raynaud, D., Jouzel, J., Fischer, H., Kawamura, K., Stocker, T.F., 2008. High-resolution carbon dioxide concentration record 650,000-800,000 years before present. Nature 453, 379–382.
Maher, B.A., Karloukovski, V.V., Mutch, T.J., 2004. High-field remanence properties of synthetic and natural submicrometre haematites and goethites: significance for environmental contexts. Earth Planet Sci. Lett. 226, 491–505.
Maher, B.A., Thompson, R., 1991. Mineral magnetic record of the Chinese loess and palaeosols. Geology 19, 3–6.
Muri, H., Berger, A., Yin, Q.Z., Voldoire, A., Salas, D., Sundaram, S., 2012. SST and ice sheet impacts on the MIS-13 climate. Clim. Dynam. 39, 1739–1761. https://doi.org/10.1007/s00382-011-1216-9.
Marković, S.B., Hambach, U., Catto, N., Jovanović, M., Buggle, B., Machalett, B., Zöller, L., Glaser, B., Frechen, M., 2009. Middle and late pleistocene loess sequences at batajnica, vojvodina, Serbia. Quat. Bar Int. 198, 255–266.
Marković, S.B., Hambach, U., Stevens, T., Kukla, G.J., Heller, F., McCoy, W.D., Oches, E.A., Buggle, B., Zöller, L., 2011. The last million years recorded at the Stari Slankamen (Northern Serbia) loess-palaeosol sequence: revised chronostratigraphy and long-term environmental trends. Quat. Sci. Rev. 30, 1142–1154.
Marković, S.B., Hambach, U., Stevens, T., Jovanoviä, M., O'Hara-Dhand, K., Basarin, B., Lu, H.Y., Smalley, I., Buggle, B., Zech, M., Svirčev, Z., Sümegi, P., Milojković, N., Zöller, L., 2012. Loess in the vojvodina region (northern Serbia): an essential link between European and Asian pleistocene environments. Neth. J. Geosci. 91, 173–188.
Marković, S.B., Stevens, T., Kukla, G.J., Hambach, U., Fitzsimmons, K.E., Gibbard, P., Buggle, B., Zech, M., Guo, Z.T., Hao, Q.Z., Wu, H.B., O'Hara Dhand, K., Smalley, I., Újvári, G., Sümegi, P., Timar-Gabor, A., Veres, D., Sirocko, F., Jary, Z., Svensson, A., Jović, V., Kovács, J., Zvirčev, Z., Vasiljević, D.A., 2015. Danube loess stratigraphytowards a pan-European loess stratigraphic model. Earth Sci. Rev. 148, 228–258.
Nie, J.S., Song, Y.G., King, J.W., Fang, X.M., Heil, C., 2010. HIRM variations in the Chinese red-clay sequence: insights into pedogenesis in the dust source area. J. Asian Earth Sci. 38, 96–104.
Rossignol-Strick, M., Paterne, M., Bassinot, F.C., Emeis, K.C., De Lange, G.J., 1998. An unusual mid-Pleistocene monsoon period over Africa and Asia. Nature 392, 269–272.
Schwertmann, U., 1971. Transformation of hematite to goethite in soils. Nature 232, 624–625.
Schwertmann, U., 1993. Relations between iron oxides, soil color, and soil formation. In: In: Bigham, J.M., Ciolkosz, E.J., Luxmoore, R.J. (Eds.), Soil Solor. SSSA Special Publications, vol. 31. pp. 51–70.
Schwertmann, U., Murad, E., 1983. Effect of pH on the formation of goethite and hematite from ferrihydrite. Clay Clay Miner. 31, 277–284.
Shi, P.H., Yang, T.B., Tian, Q.C., Jiang, S., Fan, Z., Wang, J.Y., 2013. Loess record of climatic changes during MIS 12–10 in the Jingyuan section, northwestern Chinese Loess Plateau. Quat. Bar Int. 296, 149–159.
Singer, M.J., Verosub, K.L., Fine, P., TenPas, J., 1996. A conceptual model for the enhancement of magnetic susceptibility in soils. Quat. Bar Int. 34–36, 243–248.
Sun, Y.B., Chen, J., Clemens, S.C., Liu, Q.S., Ji, J.F., Tada, R., 2006a. East Asian monsoon variability over the last seven glacial cycles recorded by a loess sequence from the northwestern Chinese Loess Plateau. Geochem. Geophys. Geosyst 7, 97–112.
Sun, Y.B., Clemens, S.C., An, Z.S., Yu, Z.W., 2006b. Astronomical timescale and palaeoclimatic implication of stacked 3.6-Myr monsoon records from the Chinese Loess Plateau. Quat. Sci. Rev. 25, 33–48.
Sun, Y.B., Wang, X.L., Liu, Q.S., Clemens, S.C., 2010. Impacts of post-depositional processes on rapid monsoon signals record by the last glacial loess deposits of northern China. Earth Planet Sci. Lett. 289, 171–179.
Thompson, R., Oldfield, F., 1986. Environmental Magnetism. Allen & Unwin, London, pp. 1–153.
Torrent, J., Liu, Q.S., Bloemendal, J., Barrón, V., 2007. Magnetic enhancement and iron oxides in the upper Luochuan loess–paleosol sequence, Chinese Loess Plateau. Soil Sci. Soc. Am. J. 71, 1570–1578.
Torrent, J., Liu, Q.S., Barron, V., 2010. Magnetic susceptibility changes in relation to pedogenesis in a Xeralf chronosequence in northwestern Spain. Eur. J. Soil Sci. 61, 161–173.
Tramp, K.L., Soreghan, G.S., Elmore, R.D., 2004. Paleoclimatic inferences from paleopedology and magnetism of the Permian Maroon Formation loessite, Colorado, USA. Geol. Soc. Amer. Bull. 116, 671–686.
Vidic, N.J., Verosub, K.L., 1999. Magnetic properties of soils of the Ljubljana Basin chronosequence, Slovenia. Chin. Sci. Bull. 44 (Suppl. 1), 75–80.
Vidic, N.J., Singer, M.J., Verosub, K.L., 2004. Duration dependence of magnetic susceptibility enhancement in the Chinese loess–palaeosols of the past 620 ky. Palaeogeogr. Palaeoclimatol. Palaeoecol. 211, 271–288.
Xiao, L.J., An, Z.S., 1999. Three large shifts in East Asian monsoon circulation indicated by loess-paleosol sequences in China and late Cenozoic deposits in Japan. Palaeogeogr. Palaeoclimatol. Palaeoecol. 154, 179–189.
Yin, Q.Z., Berger, A., Driesschaert, E., Goosse, H., Loutre, M.F., Crucifix, M., 2008. The Eurasian ice sheet reinforces the East Asian summer monsoon during the interglacial 500,000 years ago. Climate Past 4, 79–90.
Yin, Q.Z., Berger, A., Crucifix, M., 2009. Individual and combined effects of ice sheets and precession on MIS-13 climate. Climate Past 5, 229–243.
Zhou, L.P., Oldfield, F., Wintle, A.G., Robinson, S.G., Wang, J.T., 1990. Partly pedogenic origin of magnetic variations in Chinese loess. Nature 346, 737–739.